

Coordination Chemistry and Mechanisms of Metal-Catalyzed CC-Coupling Reactions. 10.[†] Ligand Dissociation in Rhodium-Catalyzed Hydroformylation: A Theoretical Study[‡]

Rochus Schmid,[§] Wolfgang A. Herrmann,^{*,§,||} and Gernot Frenking^{*,⊥}

Anorganisch-chemisches Institut der Technischen Universität München, Lichtenbergstrasse 4, D-85747 Garching, Germany, and Fachbereich Chemie der Universität Marburg, Hans-Meerwein-Strasse, D-35032 Marburg, Germany

Received July 9, 1996[Ⓞ]

The equilibrium structures of rhodium complexes $\text{HRh}(\text{CO})_n(\text{PR}_3)_{4-n}$ and $\text{HRh}(\text{CO})_n(\text{PR}_3)_{3-n}$ with $n = 1-3$ and $\text{R} = \text{H}$ have been calculated using density functional theory (DFT) with both local and gradient-corrected functionals. These molecules are model systems for the analogous complexes with $\text{R} = \text{alkyl}$ or aryl involved in homogeneously catalyzed hydroformylation, the largest scale organometallic catalysis known to date. For the compounds with $n = 1$ and $n = 2$, *ab initio* calculations at the HF and MP2 level of theory have been performed as well. Basis sets of valence double- ζ plus polarization quality were used, and in the case of the *ab initio* calculations effective core potentials for rhodium and phosphorus were applied. The ligand dissociation energies derived from single-point CCSD(T) calculations revealed that MP2 strongly overestimates bond strengths for these systems. The DFT calculations using gradient-corrected functionals yielded values very close to the CCSD(T) energies. Comparison with experimental results for PPh_3 complexes shows that the phosphine dissociation energies are calculated too low when PH_3 serves as the model phosphine. The situation is improved significantly when PMe_3 is used instead: the dissociation energy is 7.2 kcal/mol larger than for PH_3 ($n = 1$).

Introduction

Ligand dissociation energies of transition-metal (TM) complexes are difficult to determine accurately by theoretical methods. This is mainly due to the importance of electron correlation for the metal–ligand bond energy and for the structural relaxation of the remaining transition-metal fragment. The inclusion of electron correlation significantly increases the computational effort. Thus, the treatment of transition-metal systems has become feasible only when the number of electrons included in the calculation is reduced by employing effective core potentials (ECP) which replace the core electrons of the TM atoms.¹ In recent years, density functional theory (DFT) has evolved into another important method for treating systems containing transition metals, since it includes electron correlation in an approximate way for the computational costs of Hartree–Fock (HF) calculations.² On the other hand, DFT calculations lack the ability to improve the accuracy systematically by increasing the theoretical level in a stepwise manner. To benchmark the theoretical methods, the first CO dissociation energies of the zerovalent

carbonyl complexes of the chromium, iron, and nickel triads have been calculated in various studies, and they were compared with the available experimental gas-phase data.³

In homogeneous catalysis ligand dissociation steps are of prime and pivotal importance. In contrast to the above-mentioned gas-phase CO dissociation, the size of systems of practical interest is usually much larger and the dissociation takes place in the condensed phase. An example is the rhodium-catalyzed hydroformylation of terminal olefins, which is the largest scale industrial homogeneous catalytic process known.⁴ The catalyst $\text{HRh}(\text{CO})(\text{PPh}_3)_3$ (**1**) exhibits an increased selectivity toward the straight-chain aldehyde, as compared to the hydridorhodium carbonyl systems.⁵ However, this regioselectivity depends largely on the CO pressure and the phosphine concentration.^{5a} The commonly accepted dissociative mechanism⁶ is shown in Scheme 1: the catalytically active species are square-planar 16-electron complexes, formed by CO or phosphine dissociation from

[†] Part 9: Herrmann, W. A.; Elison, M.; Fischer, J.; Köcher, Ch.; Artus, G. R. *J. Angew. Chem.* **1995**, *107*, 2602; *Angew. Chem., Int. Ed. Engl.* **1995**, *34*, 3005.

[‡] In memoriam Hidemasa Takaya, † Oct. 4, 1995.

[§] Technische Universität München.

^{||} Telefax: +49 89 2891-3473. E-mail: herrmann@zaphod.anorg.chemie.tu-muenchen.de.

[⊥] Universität Marburg.

[Ⓞ] Abstract published in *Advance ACS Abstracts*, January 15, 1997.

(1) (a) Szasz, L. *Pseudopotential Theory of Atoms and Molecules*; Wiley: New York, 1985. (b) Krauss, M.; Stevens, W. J. *Annu. Rev. Phys. Chem.* **1984**, *35*, 357.

(2) (a) Labanowski, J.; Andzelm, J. *Density Functional Methods in Chemistry*; Springer-Verlag: Heidelberg, Germany, 1991. (b) Ziegler, T. *Chem. Rev.* **1991**, *91*, 651.

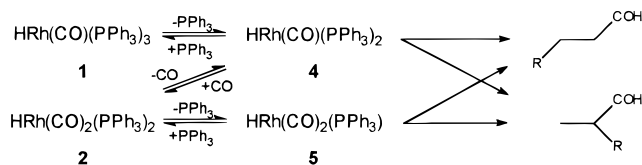
(3) (a) Ehlers, A. W.; Frenking, G. *J. Chem. Soc., Chem. Commun.* **1993**, 1709. (b) Ehlers, A. W.; Frenking, G. *J. Am. Chem. Soc.* **1994**, *116*, 1514. (c) Ehlers, A. W.; Frenking, G. *Organometallics* **1995**, *14*, 423. (d) Ehlers, A. W.; Dapprich, S.; Vyboishchikov, S. F.; Frenking, G. *Organometallics* **1996**, *15*, 105. (e) Li, J.; Schreckenbach, G.; Ziegler, T. *J. Am. Chem. Soc.* **1995**, *117*, 486.

(4) (a) Cornils, B. In *New Syntheses with Carbon Monoxide*; Falbe, J., Ed.; Springer-Verlag: New York, 1980; pp 1–225. (b) Cornils, B.; Herrmann, W. A. *Applied Homogeneous Catalysis with Organometallic Complexes*; VCH: Weinheim, Germany, 1996.

(5) (a) Evans, D.; Osborn, J. A.; Wilkinson, G. *J. Chem. Soc. A* **1968**, 3133. (b) Pruet, R. L.; Smith, J. A. *J. Org. Chem.* **1969**, *34*, 327. (c) Yagupsky, G.; Brown, C. K.; Wilkinson, G. *J. Chem. Soc. A* **1970**, 1392. (d) Brown, C. K.; Wilkinson, G. *J. Chem. Soc. A* **1970**, 2753.

(6) Tolman, C. A.; Faller, J. W. In *Homogeneous Catalysis with Metal Phosphine Complexes*; Pignolet, L. H., Ed.; Plenum: New York, 1983; pp 81–109.

Scheme 1. Simplified Dissociative Mechanism of Rhodium-Catalyzed Propene Hydroformylation Indicating the Dissociation Equilibria Involved



$\text{HRh}(\text{CO})_2(\text{PPh}_3)_2$ (**2**); the latter compound is the predominant species under a CO/H_2 atmosphere.⁷ The subsequent steps of olefin coordination and insertion lead to either a linear or a branched alkyl complex. These steps determine the isomer ratio of the product, since the following CO insertion is known to be quasi-irreversible.^{6,8} An increased steric strain in the metal coordination sphere favors the formation of linear over branched insertion products. Thus, **4** yields a higher linear-to-branched aldehyde ratio than **5** (PPh_3 is sterically much more demanding than CO). A greater phosphine concentration or a lower CO pressure leads to a higher equilibrium concentration of **4** compared to **5** and, therefore, to a higher overall selectivity, as is observed experimentally.⁶ As a consequence, the relative carbon monoxide-to-phosphine dissociation energy of **2** is of prime importance in modeling the processes responsible for the regiochemistry in propene hydroformylation on a molecular level.

General problems of hydroformylation have been subject to a variety of theoretical studies. Ziegler and co-workers have investigated the catalytic cycle of the hydroformylation of ethylene with hydridocobalt carbonyl catalysts ($\text{HCo}(\text{CO})_4$) by DFT calculations in a series of publications.⁹ The structural and electronic situation of hydridocarbonylcobalt complexes was also studied by Antolovich and Davidson by means of *ab initio* calculations.¹⁰ Apart from empirical molecular mechanics calculations, focusing on the steric demands of different chelating bisphosphine ligands,¹¹ the only theoretical investigations on rhodium phosphine systems were carried out by Morokuma and co-workers with *ab initio* methods.¹² This work was, however, restricted to the less selective catalytic pathway via **5** using PH_3 as a model phosphine ligand. All geometry optimizations were performed on the HF level of theory with a rather small basis set.^{12b} Nevertheless, the results of the study give a very valuable insight into

the nature of the transition state of olefin insertion, which is the product-determining step.

It is the aim of the present work to investigate the dissociation processes of the hydroformylation reaction in detail by *ab initio* and DFT calculations, using PH_3 as a model for the organophosphine ligand in the first approach. The results are compared with the available experimental data in order to estimate which approximations can be made and how accurately the molecular processes involved can be modeled by theoretical methods. We expect an answer to the question of whether the parent ligand PH_3 can be employed as a simplified model of organophosphorus ligands in theoretical studies concerning catalytic processes.

Computational Details

a. *Ab initio* Calculations. In all *ab initio* calculations valence double- ζ plus polarization basis sets for all non-hydrogen atoms and for the hydride were employed, which was shown to be adequate for this kind of calculation.¹³ For the rhodium atom a pseudorelativistic small-core ECP treating the valence and subvalence electrons ($(n-1)s^2$ and $(n-1)p^6$) explicitly was utilized.¹⁴ To further reduce the computational effort, a 10-electron ECP was used also for phosphorus.¹⁵ The corresponding valence basis sets were used in the following contraction schemes: (441/2111/31) for rhodium¹⁴ and (31/31/1) for phosphorus¹⁵ (in the latter case one d function with an exponent of 0.34 according to Huzinaga¹⁶ was added). For all other atoms a 6-31G(d) basis set was utilized.¹⁷ For the hydride atom the basis set was augmented by a p-type polarization function (6-31G(dp) basis set¹⁷). Since the basis set was kept the same throughout this work, we do not explicitly refer to it in the further discussion.

All geometries were optimized by analytical gradient techniques at the spin-restricted Hartree-Fock (HF) and MP2 levels of theory (Møller-Plesset perturbation theory terminated at the second order¹⁸). The HF geometries were checked to be true minima on the potential energy surface by calculating the second energy derivative matrix. Improved total energies were calculated using the MP2-optimized geometries at the CCSD(T) level of theory (coupled cluster method¹⁹ with single and double excitations and a perturbative estimate of triple excitations²⁰), with the 1s electrons of carbon and oxygen kept frozen (denoted as CCSD(T)/MP2). All optimizations and vibrational analyses were performed with the TURBOMOLE program package.²¹ The CCSD(T) single-point energies were calculated with the program ACES II.²² Since both programs are able to use molecular symmetry efficiently, the maximum possible number of symmetry elements was used, which is

(7) Evans, D.; Yagupsky, G.; Wilkinson, G. *J. Chem. Soc. A* **1968**, 2660.

(8) Pino, P. *J. Organomet. Chem.* **1980**, 200, 223.

(9) (a) Versluis, L.; Ziegler, T.; Baerends, E. J.; Ravenek, W. J. *J. Am. Chem. Soc.* **1989**, 111, 2018. (b) Versluis, L.; Ziegler, T. *Organometallics* **1990**, 9, 2985. (c) Versluis, L.; Ziegler, T.; Fan, L. *Inorg. Chem.* **1990**, 29, 4530. (d) Versluis, L.; Ziegler, T. *J. Am. Chem. Soc.* **1990**, 112, 2985. (e) Ziegler, T. *Pure Appl. Chem.* **1991**, 63, 873. (f) Ziegler, T.; Versluis, L. *Adv. Chem. Ser.* **1992**, No. 230, 75. (g) Ziegler, T.; Cavallo, L.; Bércecs, A. *Organometallics* **1993**, 12, 3586.

(10) (a) Antolovich, D.; Davidson, E. R. *J. Am. Chem. Soc.* **1987**, 109, 977. (b) Antolovich, D.; Davidson, E. R. *J. Am. Chem. Soc.* **1987**, 109, 5828. (c) Antolovich, D.; Davidson, E. R. *J. Chem. Phys.* **1988**, 88, 4967.

(11) (a) Casey, C. P.; Whiteker, G. T. *Isr. J. Chem.* **1990**, 30, 299. (b) Casey, C. P.; Whiteker, G. T.; Melville, M. G.; Petrovich, L. M.; Gavney, J. A., Jr.; Powell, D. R. *J. Am. Chem. Soc.* **1992**, 114, 5535. (c) Casey, C. P.; Petrovich, L. M. *J. Am. Chem. Soc.* **1995**, 117, 6007.

(12) (a) Ding, Y. B.; Koga, N.; Morokuma, K. *Abstracts*, 37th Symposium on Organometallic Chemistry, Osaka, Japan, 1990; Kinki Chemical Society: Osaka, Japan, 1990; Paper PA 106. (b) Koga, N.; Jin, S. Q.; Morokuma, K. *J. Am. Chem. Soc.* **1988**, 110, 3417. (c) Musaev, D. G.; Matsubara, T.; Mebel, A. M.; Koga, N.; Morokuma, K. *Pure Appl. Chem.* **1995**, 67, 257.

(13) Frenking, G.; Antes, I.; Boehme, M.; Dapprich, S.; Ehlers, A. W.; Jonas, V.; Neuhaus, A.; Otto, M.; Stegmann, R.; Veldkamp, A.; Vyboishchikov, S. F. In *Reviews in Computational Chemistry*; VCH: New York, 1996; Vol. 8, p 63.

(14) Hay, P. J.; Wadt, W. R. *J. Chem. Phys.* **1985**, 82, 299.

(15) Bergner, A.; Dolg, M.; Küchle, W.; Stoll, H.; Preuss, H. *Mol. Phys.* **1993**, 80, 1431.

(16) Huzinaga, S. *Gaussian Basis Sets for Molecular Calculations*; Elsevier: Amsterdam, 1984.

(17) (a) Ditchfield, R.; Hehre, W. J.; Pople, J. A. *J. Chem. Phys.* **1971**, 54, 724. (b) Hehre, W. J.; Ditchfield, R.; Pople, J. A. *J. Chem. Phys.* **1972**, 56, 2257. (c) Francl, M. M.; Pietro, W. J.; Hehre, W. J.; Binkley, J. S.; Gordon, M. S.; Defrees, D. J.; Pople, J. A. *J. Chem. Phys.* **1982**, 77, 3654.

(18) (a) Møller, C.; Plesset, M. S. *Phys. Rev.* **1934**, 46, 618. (b) Binkley, J. S.; Pople, J. A. *Int. J. Quantum Chem.* **1975**, 9, 229.

(19) Cizek, J. *J. Chem. Phys.* **1966**, 45, 4256.

(20) (a) Pople, J. A.; Krishnan, R.; Schlegel, H. B.; Binkley, J. S. *Int. J. Quantum Chem.* **1978**, 14, 545. (b) Bartlett, R. J.; Purvis, G. D. *Int. J. Quantum Chem.* **1978**, 14, 561. (c) Purvis, G. D.; Bartlett, R. J. *J. Chem. Phys.* **1982**, 76, 1910. (d) Raghavachari, K.; Trucks, G. W.; Pople, J. A.; Head-Gordon, M. *Chem. Phys. Lett.* **1989**, 157, 479. (e) Bartlett, R. J.; Watts, J. D.; Kucharski, S. A.; Noga, J. *Chem. Phys. Lett.* **1990**, 165, 513.

justified by the vibrational frequency calculations (no imaginary frequencies).

The accuracy of dissociation energies calculated at that level of theory (CCSD(T)/MP2) and with the types of small-core ECPs and basis sets used in this work is discussed in detail in refs 3a–d and 13. For the same reasons as outlined in these references, we did not correct the calculated dissociation energies for the basis set superposition error (BSSE), since it would leave the basis set incompleteness error (BSIE) uncorrected, which has the opposite sign of the BSSE.

b. DFT Calculations. To allow a comparison with the *ab initio* results, a valence double- ζ plus polarization basis set was used for the DFT calculations as well (except for the hydrogen atoms of phosphine). This DZVP basis set together with the A1 set of auxiliary fitting functions for the density and exchange-correlation potential is optimized especially for DFT calculations to reduce the basis set superposition error.²³ The contractions are as follows: (633321/53211/531) for rhodium, (6321/521/1) for phosphorus, (621/41/1) for carbon and oxygen, and (41) for hydrogen. In analogy to the *ab initio* calculations the basis set of the hydride atom was augmented by a polarization function (DZVP2 basis: 41/1). Because of the efficiency of DFT calculations it was not necessary to use pseudopotentials (PP). Thus, the all-electron calculations do not account for relativistic effects. For the late-second-row transition metals relativistic effects are modest, however, which was shown, for example, by Ziegler for the first CO dissociation energies of Mo(CO)₆, Ru(CO)₅, and Pd(CO)₄ (energy difference between nonrelativistic and quasi-relativistic results 1.5, 3.3, and 1.4 kcal/mol, respectively).^{3e}

All structures were optimized without any restrictions on the LDA (local density approximation) level of theory by analytical gradient techniques (the corresponding energies are denoted as LDA/LDA).²⁴ These geometries were verified to be minima on the potential energy surface by analytical calculation of the second energy derivative matrix.²⁵ A subset of structures was further optimized, including the gradient-corrected exchange functional according to Becke²⁶ and correlation functional according to Perdew²⁷ in a self-consistent way (denoted as NLDA/NLDA). This is known to improve the calculated values of metal–ligand bond lengths.^{2b} Total energies, however, have already been calculated with a reasonable accuracy by utilizing a perturbative inclusion of gradient corrections using the LDA geometry and density (denoted as NLDA/LDA).²⁸ All DFT calculations were performed with the program DGauss²⁹ using the UNICHEM interface.³⁰

Results and Discussion

a. Geometries. Five-coordinate rhodium(I) complexes are known to undergo rapid conversion between different isomers (Berry pseudorotation and related

mechanisms³¹). To keep the number of calculations within a reasonable framework, only trigonal-bipyramidal (tbp) structures with an axial hydrido ligand have been considered. These conformations are known from experiment and theory to be more stable than those with an equatorial hydride.³² The four-coordinate complexes were assumed to have square-planar (sp) structures, as expected for rhodium(I) with a d⁸ electron configuration. For HRh(CO)_n(PH₃)_{4–n} with *n* = 1–3 and HRh(CO)_n(PH₃)_{3–n} with *n* = 1, 2, two isomers are possible. All molecules were optimized at the LDA level of theory. From a structure with the highest possible symmetry as the starting point, transition states with respect to a rotation of the phosphine fragment around the Rh–P bond were found in certain cases. These structures were reoptimized with a reduced symmetry until a true minimum (no imaginary frequency) was located. It should be noted that this does not necessarily lead to the global minimum on the potential energy surface. However, since the energy differences between the transition states and the minimum are on the order of fractions of kilocalories per mole, the energy profile of this rotation can be considered to be very shallow. The final molecular structure data together with the relative LDA/LDA and NLDA/LDA energies (see Computational Details) of the isomers are shown in Figures 1 and 2.

The angle between the hydride and the adjacent ligands is smaller than 90° throughout, even though no severe steric congestion is present. The deviation is about 10° from the value found in an ideal tbp or sp structure. In contrast to all other sp complexes, **5b** and **6** show a nonplanar energy minimum halfway between a pseudo-trigonal-bipyramidal and a square-planar structure (Figure 3). In both cases, the two CO ligands avoid the trans arrangement in the square-planar structure. Previous calculations on **5b** at the HF level of theory gave a planar energy minimum geometry.^{12b} Apart from these deviations, all complexes have the expected tbp or sp minimum structures. The metal–ligand bond lengths are governed by two major effects. (i) The well-known trans influence leads e.g. to a shortening of the Rh–H bond, when a carbonyl ligand (**1a**, **2a**, **3a**, **4a**, **5a**) is replaced by a phosphine (**1b**, **2b**, **3b**, **4b**, **5b**) in the trans position. (ii) In both series of tbp and sp complexes the successive replacement of a carbonyl by a phosphine ligand leads to an increase of the Rh–H bond length, whereas the Rh–P and Rh–C bond lengths decrease. This can be rationalized by the following consideration: phosphine is a weaker π -acceptor and a stronger σ -donor compared to the carbonyl ligand. Thus, increasing the number of phosphine ligands results in an increased electron density at the metal center. Consequently, the Rh–H bond length increases since the hydride ligand is merely a σ -donor. On the other hand both PH₃ and CO are not only σ -donor but also π -acceptor ligands. An increasing electron density at the metal atom enlarges the back-donation to these ligands, resulting in decreasing Rh–P and Rh–C bond lengths. These tendencies are also shown by the Löwdin net atomic charges of rhodium

(21) (a) Häser, M.; Ahlrichs, R. *J. Comput. Chem.* **1989**, *80*, 104. (b) Ahlrichs, R.; Bär, M.; Häser, M.; Horn, H.; Kölmel, M. C. *Chem. Phys. Lett.* **1989**, *162*, 165. (c) Horn, H.; Weiss, H.; Häser, M.; Ehring, M.; Ahlrichs, R. *J. Comput. Chem.* **1991**, *12*, 1058. (d) Häser, M.; Almlöf, J.; Feyereisen, M. W. *Theor. Chim. Acta* **1991**, *79*, 115. (e) Schäfer, A.; Horn, H.; Ahlrichs, R. *J. Chem. Phys.* **1992**, *97*, 2571. (f) Häser, M.; Ahlrichs, R.; Baron, H. P.; Weiss, P.; Horn, H. *Theor. Chim. Acta* **1992**, *83*, 455.

(22) ACES II, an *ab initio* program written by J. F. Stanton, J. Gauss, J. D. Watts, W. J. Lauderdale, and R. J. Bartlett, University of Florida, Gainesville, FL, 1991.

(23) Godbout, N.; Salahub, D. R.; Andzelm, J.; Wimmer, E. *Can. J. Chem.* **1992**, *70*, 560.

(24) Fournier, R.; Andzelm, J.; Salahub, D. R. *J. Chem. Phys.* **1989**, *90*, 6371.

(25) Komornicki, A.; Fitzgerald, G. *J. Chem. Phys.* **1993**, *98*, 1398.

(26) Becke, A. *Phys. Rev.* **1988**, *A38*, 3098.

(27) Perdew, J. P. *Phys. Rev.* **1986**, *B33*, 8822; **1986**, *B34*, 7406.

(28) (a) Fan, L.; Ziegler, T. *J. Chem. Phys.* **1991**, *94*, 6057. (b) Lee, C.; Fitzgerald, G.; Yang, W. *J. Chem. Phys.* **1993**, *98*, 2971.

(29) Andzelm, J.; Wimmer, E. *J. Chem. Phys.* **1992**, *96*, 1280.

(30) UniChem 2.3.1, Cray Research Inc., 1994.

(31) Meakin, P.; Muetterties, E. L.; Jesson, J. P. *J. Am. Chem. Soc.* **1972**, *94*, 5271.

(32) (a) Frenz, B. A.; Ibers, J. A. In *The Hydride Series*; Muetterties, E. L., Ed.; Marcel Dekker: New York, 1971; Vol. I, Chapter III. (b) Rossi, A. R.; Hoffmann, R. *Inorg. Chem.* **1975**, *14*, 365.

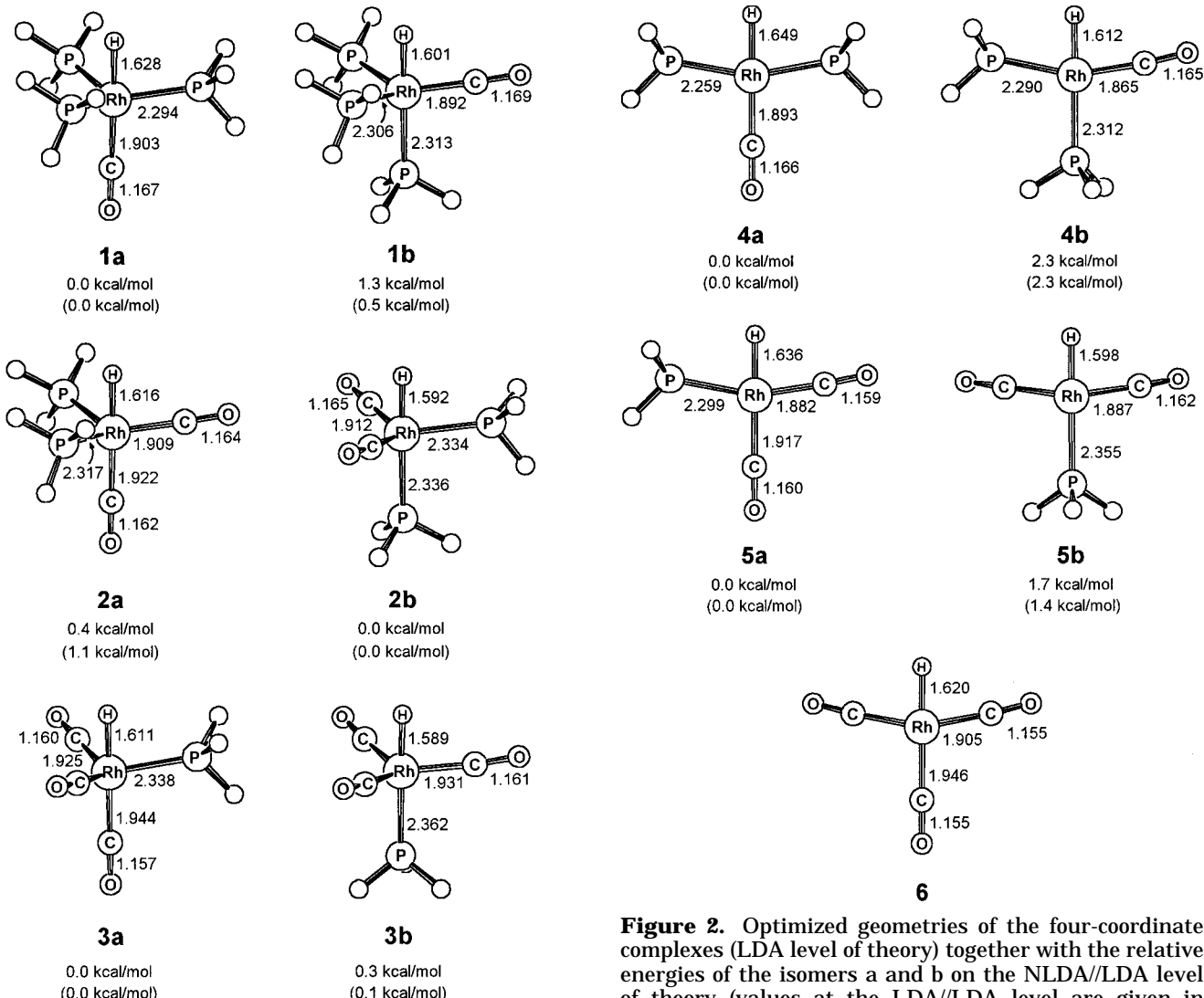


Figure 1. Optimized geometries of the five-coordinate complexes (LDA level of theory) together with the relative energies of the isomers a and b on the NLDA/LDA level of theory (values at the LDA/LDA level are given in parentheses). Bond lengths are given in angstroms.

given in Table 1. The 16-electron complexes generally possess a lower negative charge on rhodium compared to their 18-electron counterparts.

The energy differences (NLDA/LDA and LDA/LDA) between the different isomers of the *tbp* complexes are rather small, whereas the energy differences of the *sp* isomers are slightly more pronounced, at 2.3 and 1.7 kcal/mol for **4a,b** and **5a,b**, respectively. For the computationally more expensive optimizations on the NLDA level of theory, four structures (**1a**, **2a**, **4a**, and **5a**) were selected because of their relevance in the hydroformylation reaction and their relative stability. **2a** was chosen, despite its slightly lower stability compared to **2b**, because the analogous PPh_3 complexes are known to prefer the diequatorial arrangement for steric reasons (measured by NMR spectroscopy at room temperature³³). Experimentally known are the crystal structures of **1** (PPh_3 ligands)³⁴ and **4** (tricyclohexylphosphine ligands),³⁵ both possessing the conformations

Figure 2. Optimized geometries of the four-coordinate complexes (LDA level of theory) together with the relative energies of the isomers a and b on the NLDA/LDA level of theory (values at the LDA/LDA level are given in parentheses). Bond lengths are given in angstroms.

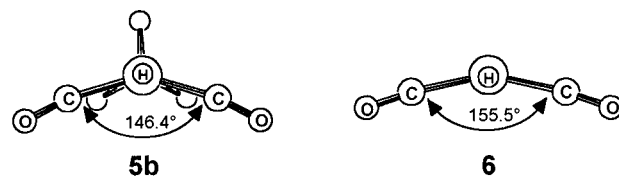


Figure 3. Deviation from a square-planar structure of the complexes **5b** and **6**.

Table 1. Löwdin Net Atomic Charges on Rhodium (LDA Level of Theory)

	1	2	3	4	5	6
a	-1.318	-1.074	-0.826	-1.021	-0.744	-0.461
b	-1.328	-1.058	-0.830	-1.028	-0.687	

of **1a** and **4a**, respectively. In order to verify the results of the DFT methods, the same set was also optimized by *ab initio* methods at the HF and MP2 levels of theory. The structural results of these calculations are given in Table 2 and 3 together with the available experimental data.

The structural differences between the LDA and NLDA minima are modest. As a result of the known

(33) Brown, J. M.; Kent, A. G. *J. Chem. Soc., Perkin Trans. 2* **1987**, 1597.

(34) (a) La Placa, S. J.; Ibers, J. A. *Acta Crystallogr.* **1965**, *18*, 511. (b) Babra, I. S.; Morley, L. S.; Nyburg, S. C.; Parkins, A. W. *J. Cryst. Spectrosc.* **1993**, *23*, 997.

(35) Freeman, M. A.; Young, D. A. *Inorg. Chem.* **1986**, *25*, 1556.

Table 2. Calculated Structural Data for Five-Coordinate Complexes 1a and 2a^a

	1a				1 exptl	2a			
	HF	MP2	LDA	NLDA		HF	MP2	LDA	NLDA
Rh–H (Å)	1.615	1.589	1.628	1.635	1.61 ^b	1.604	1.581	1.616	1.622
Rh–P _{eq} (Å)	2.441	2.304	2.294	2.348	2.33 ^b	2.494	2.337	2.317	2.379
Rh–C _{eq} (Å)						1.993	1.884	1.909	1.945
Rh–C _{ax} (Å)	2.035	1.897	1.903	1.946	1.83 ^b	2.059	1.925	1.922	1.967
C–O _{eq} (Å)						1.120	1.170	1.164	1.170
C–O _{ax} (Å)	1.119	1.175	1.167	1.173	1.17 ^b	1.116	1.168	1.162	1.168
H–Rh–P _{eq} (deg)	82.3	84.6	80.2	80.4	81 ^c	82.3	81.5	80.8	82.0
H–Rh–C _{eq} (deg)						82.0	82.7	81.5	80.9
H–Rh–P/C _{ax} (deg)					<i>d</i>	179.8	179.0	179.3	178.2

^a The subscripts eq and ax denominate equatorial and axial ligand positions. ^b Average values from both crystal structure analyses.³⁴ ^c Estimated by 180° minus angle (C_{ax}–Rh–P_{eq}). ^d Angle cannot be given because of missing or unreliable hydride position.³⁴

Table 3. Calculated Structural Data for Four-Coordinate Complexes 4a and 5a^a

	4a				4 exptl	5a			
	HF	MP2	LDA	NLDA		HF	MP2	LDA	NLDA
Rh–H (Å)	1.631	1.621	1.649	1.659	1.72	1.629	1.602	1.636	1.640
Rh–P _{ci} (Å)	2.393	2.278	2.259	2.305	2.294 ^b	2.411	2.343	2.299	2.364
Rh–C _{ci} (Å)						1.981	1.856	1.882	1.915
Rh–C _{tr} (Å)	2.029	1.864	1.893	1.934	1.858	2.056	1.910	1.917	1.958
C–O _{ci} (Å)						1.116	1.165	1.159	1.166
C–O _{tr} (Å)	1.119	1.177	1.166	1.173	1.136	1.115	1.167	1.160	1.166
H–Rh–P _{ci} (deg)	83.6	83.5	79.6	79.9	82 ^b	80.3	79.4	79.2	79.4
H–Rh–C _{ci} (deg)						82.1	82.8	80.8	81.3
H–Rh–P/C _{tr} (deg)					178.5	179.1	180.0	180.0	179.9

^a The subscripts ci and tr denominate cis and trans positions of the ligand with respect to the hydride. ^b Averaged value, since the experimental structure deviates from C_{2v} symmetry.³⁵

overestimation of bond strengths in LDA, all bond lengths are calculated to be somewhat longer at the NLDA level. The HF geometries show significantly longer Rh–P and Rh–C bond lengths. This originates from the lack of electron correlation, which is necessary to describe metal–ligand π -back-bonding. By including electron correlation at the MP2 level, the Rh–C and Rh–P bonds shrink by up to 0.14 Å. NLDA and MP2 afford very similar geometries with the metal–ligand bond lengths calculated by MP2 being slightly shorter. Apart from that, the general shapes of all complexes at the LDA, NLDA, HF, and MP2 levels are very similar.

A validation of the calculated geometries is hampered by the fact that no experimental data for the complexes with PH₃ ligands are available. The organic substituents on phosphorus in the experimentally known complexes (phenyl for **1** and cyclohexyl for **4**) give rise to deviations because of electronic (basicity) and steric effects. Furthermore, packing forces in the single-crystal and experimental uncertainties will influence the experimental results. **1** crystallizes in two isomeric forms with different rotational positions of the phenyl rings.³⁴ Only in one of the crystal structure analyses of **1** is the hydride located with a large positional uncertainty.^{34a} A direct assessment of the calculational accuracy of the different methods is therefore difficult. The absolute mean deviations between calculated Rh–P and Rh–C bond lengths of **1a** and **4a** and the experimental values of **1** and **4** respectively are as follows: MP2, 0.026 Å; NLDA, 0.038 Å; LDA, 0.041 Å; HF, 0.130 Å. Thus, MP2, NLDA, and also LDA afford reasonable geometries, whereas the HF geometries are in poor agreement with experiment. The bending of the ligands adjacent to the hydride out of the ideal t_{bp} or sp position is reproduced by all methods, and it can be concluded that this effect is not due to steric repulsions of the substituents of phosphorus in the experimental structures.

Table 4. Calculated Rh–H and C–O Stretching Frequencies of the Five-Coordinate Complexes^a

	$\nu(\text{Rh–H})$ (cm ⁻¹)	$\nu(\text{C–O})_{\text{eq}}$ (cm ⁻¹)	$\nu(\text{C–O})_{\text{ax}}$ (cm ⁻¹)
1a (LDA)	1913		2050
1a (HF)	1909		2361
1 (exptl) ^b	2000		1920
1b (LDA)	2003	2021	
2a (LDA)	1961	2043	2087
2a (HF)	1961	2345	2394
2 (exptl) ^b	2038	1939	1980
2b (LDA)	2049	2028 (a)	2061 (s)
3a (LDA)	1976	2057 (a)	2071 (s)
3b (LDA)	2056	2048 (da)	2099 (s)

^a Legend: (a) asymmetric mode; (s) symmetric mode; (da) two degenerate asymmetric modes. ^b Experimental values from ref 7.

Table 5. Calculated Rh–H and C–O Stretching Frequencies for the Four-Coordinate Complexes^a

	$\nu(\text{Rh–H})$ (cm ⁻¹)	$\nu(\text{C–O})_{\text{ci}}$ (cm ⁻¹)	$\nu(\text{C–O})_{\text{tr}}$ (cm ⁻¹)
4a (LDA)	1826		2047
4a (HF)	1804		2367
4b (LDA)	1939	2053	
5a (LDA)	1874	2108	2062
5a (HF)	1871	2412	2383
5b (LDA)	1997	2036 (a)	2095 (s)
6 (LDA)	1944	2078 (a)	2155 (s)

^a Legend: (a) asymmetric mode; (s) symmetric mode.

b. Vibrational Analysis. In the following section only the Rh–H and C–O stretching modes are discussed, since they are easily identified in experimental vibrational spectra and since they are a sensitive probe for the electronic situation of the rhodium center. The other metal–ligand stretching modes are generally coupled to metal–ligand bending modes. The vibrational analysis was performed at the LDA and HF levels of theory, as mentioned in the Computational Details (Tables 4 and 5).

Both Rh–H and C–O stretching frequencies show the trends that were already observed in the metal–ligand bond lengths. In particular, the Rh–H frequency

Table 6. Calculated Ligand Dissociation Energies without ZPE Correction

	$\Delta E_{1a-4a}(\text{PH}_3)$ (kcal/mol)	$\Delta E_{2a-4a}(\text{CO})$ (kcal/mol)	$\Delta E_{2a-5a}(\text{PH}_3)$ (kcal/mol)
HF//HF	-3.2	0.5	-3.4
MP2//HF	19.4	28.4	20.7
MP2//MP2	22.7	32.9	24.7
CCSD//MP2	10.3	18.8	10.9
CCSD(T)//MP2	11.9	21.6	12.7
LDA/LDA	27.1	39.6	28.4
NLDA/LDA	12.9	23.2	14.1
NLDA/NLDA	13.4	24.0	14.5

decreases with increasing electron density on rhodium, which means weaker bonding and thus larger bond length. A CO in a position trans to the hydride lowers this frequency in comparison to phosphine by nearly 100 cm^{-1} because of the trans influence. These general trends are also reproduced by the HF results, but the absolute values of the C–O stretching modes are too high. This is a consequence of the insufficient description of metal-to-carbonyl back-donation at the uncorrelated level, which leads to an overestimation of C–O bond strength.

In comparison to the available experimental values of hydridorhodium carbonyl compounds with triarylphosphine ligands, the Rh–H absorption is predicted too low and the CO absorption too high: **1** has a strong C–O band at 1920 cm^{-1} (**1a**, LDA: 2050 cm^{-1}), and the Rh–H absorption appears at about 2000 cm^{-1} (**1a**, LDA: 1913 cm^{-1}).⁷ The corresponding complex HRh(CO)₂(PPh₃)₂ (**2**), which is formed under a H₂/CO atmosphere, has a Rh–H band at 2038 cm^{-1} (**2a**, LDA: 1961 cm^{-1}) and two C–O bands at 1980 and 1939 cm^{-1} (**2a**, LDA: 2087 and 2043 cm^{-1}).⁷ Thus, the tendency for an increased Rh–H and C–O stretching frequency upon replacement of a phosphine by a CO ligand is observed in the experiment as well. It should be noted that solvent effects and steric and electronic differences between PPh₃ and the model PH₃ will influence the absolute values.

c. Dissociation Energies. The main focus of this work is to verify the accuracy of the theoretical methods in order to reproduce ligand dissociation energies. The results obtained so far in the literature are solely based on HF-optimized structures. The difference between HF//HF and MP2//HF PH₃ dissociation energies (**2a** → **5a**) being 1.8 and 21.4 kcal/mol, respectively,^{12a} demonstrates the necessity to include correlation effects. The experimental value of 20 ± 1 kcal/mol for the dissociation enthalpy of PPh₃ from HRh(CO)(PPh₃)₃ (**1**) measured in solution by dynamic NMR spectroscopy³⁶ seems, however, to be in good agreement with the calculated MP2//HF gas-phase dissociation energy for PH₃ dissociation from **1a**.

It was shown that CCSD(T)//MP2 dissociation energies are nearly of chemical accuracy for low-valent transition-metal complexes.^{3a–d,13} We have therefore performed CCSD(T) single-point energy calculations for **1a**, **2a**, **4a**, and **5a** at the MP2-optimized geometries to serve as benchmark results in order to validate other methods. Table 6 gives the dissociation energies at the different theoretical levels without zero-point energy (ZPE) correction.

The HF level of theory completely fails to describe the energetics of dissociation. Interestingly, the CO dissociation energy from **2a** to **4a** is about 10 kcal/mol larger than the corresponding PH₃ dissociation from **1a** to **4a** throughout. Furthermore, the dissociation of PH₃ from **2a** is always slightly more endothermic (about 1 kcal/mol) than from **1a**. These findings can be rationalized by the same arguments already set up in the discussion of geometries and vibrational frequencies. Because of its higher back-bonding ability, the CO ligand is more firmly bonded, which leads to a higher dissociation energy. For the same reason, a larger number of CO ligands reduces the electron density at the metal (see Table 1), thereby stabilizing the 18-electron complexes and destabilizing the 16-electron complexes. Thus, the dissociation energy for PH₃ increases from **1a** to **2a**.

The consistent description of the relative bond energies at correlated levels of theory and the large differences in the absolute values indicate that the major difficulty for the theoretical methods is the calculation of both the 5-fold-coordinated trigonal bipyramidal and the 4-fold-coordinated square-planar complexes with the same accuracy. As a consequence, the relative dissociation energies of any (correlated) level of theory will be much more accurate than the corresponding absolute values. This has recently been recognized in a theoretical study which introduced the concept of reaction energies for isostructural reactions.³⁷

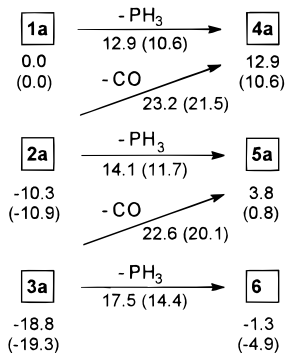
In the following section, only the PH₃ dissociation energy **1a** → **4a** will be discussed, since it serves as a model for the other dissociation processes. As already calculated by Morokuma, the MP2 dissociation energies at the HF-optimized and MP2-optimized geometries are, at 19.4 and 22.7 kcal/mol, close to the experimental value for the analogous PPh₃ dissociation in solution ($\Delta H = 20 \pm 1$ kcal/mol^{33,36}). However, a more accurate description of electron correlation with the CCSD(T) method affords a value of only 11.9 kcal/mol, indicating that MP2 overestimates the dissociation energy by about 11 kcal/mol, which is a well-known shortcoming of this theoretical approach for the treatment of dative bonds.^{3a–d,13} Since we find very small absolute values in our specific case, this deviation appears, however, to be very large. The MP2//HF value is closer to the CCSD(T) value because of error cancellation resulting from the metal–ligand bond length predicted to be too long on the HF level. As a consequence, two conclusions have to be drawn. (i) PH₃ is not suitable as a model for PPh₃ or other substituted phosphines, especially if ligand basicity plays an important role, as in the case of dissociation processes. (ii) MP2 bond energies are not appropriate for these systems as far as absolute values are concerned. The agreement between the gas-phase bond energy of PH₃ calculated at the MP2 level of theory and the corresponding experimental PPh₃ dissociation energy of HRh(CO)(PPh₃)₃ are the result of a fortuitous error cancellation.

The DFT calculations include electron correlation in an approximate way at a fraction of the computational effort needed for the post-HF methods. As already discussed, the geometries are satisfactory even at the LDA level. The binding energies, however, are over-

(36) Kastrup, R. V.; Merola, J. S.; Oswald, A. A. *Adv. Chem. Ser.* **1982**, No. 196, 43.

(37) Dapprich, S.; Pidun, U.; Ehlers, A. W.; Frenking, G. *Chem. Phys. Lett.* **1995**, 242, 521.

Scheme 2. Dissociation Cascade from 1a to 6 with the Ligand Dissociation Energies and the Relative Energy with Respect to 1a in kcal/mol (NLDA/LDA Level of Theory)^a



^a ZPE-corrected values are given in parentheses.

estimated, as known from the literature.³⁸ These deficiencies can be overcome upon inclusion of gradient corrections in the exchange correlation functional in a perturbative way (geometry and density optimized at the LDA level of theory).²⁸ Due to the shorter metal to ligand bond length at the LDA level in comparison with the NLDA level, the NLDA/LDA dissociation energies are slightly lower than the corresponding NLDA/NLDA values. The differences are not significant, however, since the LDA geometries are close to the NLDA ones. The NLDA dissociation energies of the three processes **1a** → **4a**, **2a** → **4a**, and **2a** → **5a** are in excellent agreement with the CCSD(T)//MP2 energies. Thus, NLDA-DFT calculations can be seen as a very efficient tool to study this system with adequate accuracy for the computational cost of HF calculations. It should be noted that, given the approximations made (PH₃ instead of PPh₃, no solvent and temperature effects), an exact experimental reference value is not available.

In order to reduce the computational effort further, we have also performed the DFT calculations using the pseudopotentials implemented in the program DGauss.³⁹ They include scalar relativistic effects but treat the subvalence shell of rhodium (4s and 4p) as a part of the core (large core PP). The geometries found are close to the nonrelativistic all-electron calculations, but the dissociation energies are too high (e.g. **1a** → **4a**, 18.5 kcal/mol at the NLDA/NLDA level). Thus, for the second-row transition metal rhodium, the subvalence relaxation is by far more important than relativistic effects and must not be omitted.

For further discussion we will use the DFT NLDA/LDA bond energies, since a greater number of dissociation energies are available at this level of theory. Scheme 2 shows the complete energy surface of the dissociation/association cascade from **1a** to **6**. Three points are in disagreement with the experimental results. (i) The dissociation energy of PH₃ from **1a** to **4a** is too low compared with the experimental measurement for PPh₃. (ii) **3a** is calculated to be more stable than **2a**. However, if the PPh₃ complex **1** is treated with 1 atm of CO/H₂ (to avoid the formation of a dimeric complex by loss of H₂), only one CO substitution by a phosphine is observed: **2** is the stable species under

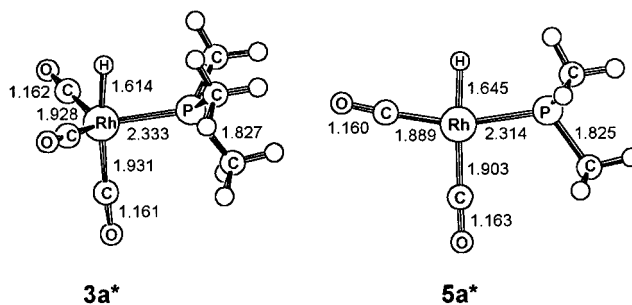


Figure 4. Optimized geometries of the PMe₃ complexes **3a*** and **5a*** (LDA level of theory). Bond lengths are given in angstroms.

these conditions.⁷ (iii) According to our calculations only the less selective PPh₃ analogue of **5a** should be present under catalytic conditions, because of the large difference between CO and phosphine dissociation energies. This is not the case in experiment, since the selectivity can be changed by orders of magnitude upon a variation of the CO to phosphine ratio. Therefore, the relative dissociation energies cannot differ so much. Assuming that PPh₃, which is known to be more basic than PH₃, would have a significantly higher dissociation energy, the theoretical results would be in much better accord with the above-mentioned experimental findings.

d. Dissociation of PMe₃. To investigate the effect of increased basicity of the phosphine on the dissociation energy, PMe₃ served as the smallest possible model ligand. The differences between PPh₃ and PMe₃ are small in comparison with the differences to PH₃. This can be estimated from the Tolman electronic factors of PH₃, PMe₃, and PPh₃ which are 2083.2, 2068.9, and 2064.1 cm⁻¹, respectively.⁴⁰ The same observation was made by Häberlen and Rösch, who have calculated the phosphine dissociation energies of Au(Me)(PR₃) at the DFT-LDA level: the PMe₃ dissociation energy (56.4 kcal/mol) is close to that of PPh₃ (58.8 kcal/mol), whereas the value for PH₃ (43.7 kcal/mol) is significantly lower.⁴¹

A full optimization of a rhodium complex with one PMe₃ ligand was feasible only at the DFT-LDA level of theory. The all-staggered conformation of the methyl groups found in the free ligand was maintained in the optimization of the complexes HRh(CO)₃(PMe₃) (**3a***) and HRh(CO)₂(PMe₃) (**5a***) starting from a phosphine rotational position similar to the equivalent PH₃ structures of **3a** and **5a**. In both cases the stationary points could not be verified as true minima by a vibrational analysis, because of the high computational costs. Figure 4 shows the geometries of **3a*** and **5a*** together with the relevant structural data.

The differences between **3a*** and **5a*** and the corresponding PH₃ complexes **3a** and **5a** are more distinct for the square-planar 16-electron compounds. The rhodium Löwdin partial charge is lower (**5a***, -0.767; **5a**, -0.744) and the Rh-P bond length is longer (**5a***, 2.314 Å; **5a**, 2.299 Å) for the PMe₃ complex. In the case of the 18-electron compounds the differences are less pronounced (Löwdin charge on rhodium: **3a***, -0.832; **3a**, -0.826; Rh-P bond length: **3a***, 2.333 Å; **3a**, 2.338 Å).

In contrast to the rather similar structural features of the PMe₃ and PH₃ complexes, the dissociation ener-

(38) Fan, L.; Ziegler, T. *J. Chem. Phys.* **1991**, *95*, 7401.

(39) Chen, H.; Kraskowski, M.; Fitzgerald, G. *J. Chem. Phys.* **1993**, *98*, 8710.

(40) Tolman, C. A. *Chem. Rev.* **1977**, *77*, 313.

(41) Häberlen, O. D.; Rösch, N. *J. Phys. Chem.* **1993**, *97*, 4970.

gies differ significantly. The NLDA/LDA dissociation energy of PMe_3 from **3a*** to **6** (24.7 kcal/mol) is 7.2 kcal/mol higher than the corresponding PH_3 dissociation energy (17.5 kcal/mol). The indirect influence of phosphorus substitution is smaller: the CO dissociation energy is reduced by only 1.3 kcal/mol (**3a*** \rightarrow **5a***, 21.3 kcal/mol; **3a** \rightarrow **5a**, 22.6 kcal/mol). As a consequence, the phosphine and CO dissociation energies become much closer and the substitution of a phosphine by a CO ligand does not continuously stabilize the complexes. If one assumes an increase of the phosphine dissociation energy by 7.2 kcal/mol and a decrease of the CO dissociation energy by 1.3 kcal/mol upon going from PH_3 to PPh_3 to be valid for the whole dissociation/association cascade (Scheme 2), **2a** and **3a** become similar in energy (1.8 kcal/mol stabilized with respect to **1a**) and also **4a** and **5a** differ by less than 1 kcal/mol in energy, which is in accord with experimental findings, as discussed in the previous section.

Conclusion

In this study, different theoretical methods and model systems for the industrially important rhodium-catalyzed hydroformylation are compared with respect to accuracy and computational efficiency. The findings revealed that geometry optimizations with uncorrelated methods can lead to wrong energy minimum structures. Furthermore, the calculated CCSD(T) bond energies, which are known to reproduce experimental dissociation energies with high accuracy, indicate that the MP2 level of theory overestimates bonding up to 100%. Accurate geometries and, in the present case, even reliable bond energies can be obtained by DFT methods employing gradient-corrected functionals at a fraction of the computational effort necessary for CCSD(T) calculations. This makes DFT methods an ideal tool to study larger systems. The calculated phosphine dissociation ener-

gies using PH_3 as a model ligand for PPh_3 are too low compared with the corresponding experimental values for PPh_3 complexes. Therefore, rhodium complexes with one PMe_3 ligand were calculated at the NLDA/LDA level of theory (**3a*** and **5a***), which yielded a 50% greater dissociation energy of PMe_3 compared with PH_3 . One can conclude that previous results for phosphine dissociation energies compared well with experimental measurements just because of error compensation resulting from both insufficient methods and model systems. At least PMe_3 must be used as a model for PPh_3 as far as dissociation energies are concerned; the parent compound PH_3 is clearly insufficient for this purpose, and one has to be extremely careful in employing it as the simplified model of catalyst-relevant organophosphines.

Further steps in the rhodium-catalyzed propene hydroformylation, which are relevant for regioselectivity, are currently being investigated theoretically in our laboratory. In addition to that, steric effects are being studied within our previously published force field approach,⁴² using the geometries which were calculated by quantum-mechanical methods.

Acknowledgment. This work has been supported by "Bayerischer Forschungsverbund Katalyse" (FOR-KAT) and the "Bundesministerium für Bildung und Forschung" (BMBF). We gratefully acknowledge excellent service by HRZ Marburg and the Leibniz-Rechenzentrum of the Bavarian Academy of Sciences in München for providing the computational facilities. We thank Dr. Martin Kaupp (Stuttgart), Dr. Matthias Wagner (München), and Dipl.-Chem. Ulrich Pidun (Marburg) for helpful discussions.

OM960562K

(42) Herrmann, W. A.; Schmid, R.; Kohlpaintner, C. W.; Priermeier, T. *Organometallics* **1995**, *14*, 1961.